Nonlinear Dyn (2021) 104:2711–2721
https://doi.org/10.1007/s11071-021-06427-x

ORIGINAL PAPER

Synchronization and chimeras in a network of photosensitive FitzHugh–Nagumo neurons

Iqtadar Hussain · Sajad Jafari · Dibakar Ghosh · Matjaž Perc

Received: 11 February 2021 / Accepted: 30 March 2021 / Published online: 9 May 2021

Abstract Recently, a photosensitive model has been proposed that takes into account nonlinear encoding and responses of photosensitive neurons that are subject to optical signals. In the model, a photocell term has been added to the well-known FitzHugh–Nagumo neuron, which results in a time-varying voltage source. The modified model exhibits most of the main characteristics of biological neurons, like spiking, bursting, and chaotic responses, but is also amenable to study the effect of optical signals. In this paper, we consider a small-world network of photosensitive neurons and study their collective behavior in dependence on interaction strength. We show that the network exhibits synchronization in a specific range of coupling strengths before transcending into a chimera state. We use the master stability function, a local-order parameter, as well as recurrence plots to verify the reported results.

Keywords Photosensitive neuron · Synchronization · Chimera · Master stability function · Recurrence plot

I. Hussain (✉)
Department of Mathematics, Statistics and Physics, Qatar University, 2713, Doha, Qatar
e-mail: iqtadarqau@gmail.com

S. Jafari
Center for Computational Biology, Chennai Institute of Technology, Chennai, India

S. Jafari
Department of Biomedical Engineering, Amirkabir University of Technology, No. 350, Hafez Ave, Valiasr Square, Tehran 159163-4311, Iran
e-mail: sajadjafari83@gmail.com

D. Ghosh
Physics and Applied Mathematics Unit, Indian Statistical Institute, 203 B. T. Road, Kolkata 700108, India
e-mail: diba.ghosh@gmail.com

M. Perc
Faculty of Natural Sciences and Mathematics, University of Maribor, Koroška cesta 160, 2000 Maribor, Slovenia

M. Perc
Department of Medical Research, China Medical University Hospital, China Medical University, Taichung 404332, Taiwan

M. Perc
Alma Mater Europaea ECM, Slovenska ulica 17, 2000 Maribor, Slovenia

M. Perc
Complexity Science Hub Vienna, Josefstädterstraße 39, 1080 Vienna, Austria e-mail: matjaz.perc@um.si

1 Introduction

Excitability, which is defined as the brain's ability to produce stimulus, is one of the most important features of nerve systems [1]. It has been investigated from both biological and computational point of view [2]. Various types of computational model of excitable neurons have been investigated in computational neuroscience [3]. One of the most well-known voltage-based neuron models is the Hodgkin–Huxley (HH) model, which has been inspired by the ionic neural system process in the squid axon [4]. This model is based on Kirchhoff's law, in which an excitable

neuron is considered as an electrical circuit. To get rid of the curse of dimensionality and difficulty in computation, the low-dimensional neuron model has been proposed, such as Hindmarsh–Rose (HR) [5] and Fitzhugh–Nagumo (FHN) [6]. The excitability of these neuron models has been investigated through different stimuli [7]. For instance, Valenti et al. [8] have investigated the excitability of the FHN exposed to colored noise. They have found that the efficiency of the neuronal response may be enhanced in the strongly correlated noise. Moreover, the excitability of FHN neuron dynamics can be affected when a neuron is subjected to an electrical field [9,10] and magnetic flow effect [11,12]. The results confirmed that neural dynamical behavior is very sensitive to both amplitude and frequency of the external field. Uzuntarla et al. [13] have reported that both excitability and input regime of the HH neuron model can be considered as a controller to the destructive influence of synaptic unreliability. Another important feature that can affect the photosensitive neurons is optical signals. Recently, Liu et al. [14] proposed a dynamical neuron model with a photoreceptor, a suitable model of photosensitive neurons. The collective behavior of the ensemble of photosensitive neurons in the form of small-world network has not been explored before, from the best of our knowledge.

After analyzing a single neuron's dynamical behavior, most of the attention has been gained to the complex patterns of the neural networks [15]. It has been shown that there might be a meaningful correlation between the collective behavior of the neural network and some functional activities of the brain. For instance, Reinhart and Nguyen reported that the brain circuits' synchronization can be the cause of the working memory [16]. Babiloni et al. [17] have claimed that Alzheimer's disease can be caused by abnormal cortical neural synchronization. Interactions circulated through the coupled neurons can result in various collective behavior such as global or local synchronization, chimera states, and spiral waves [18,19]. Global synchronization refers to the same dynamical behavior of all network agents at the same time. There can be found many related types of research in the literature which have covered both analytical and simulation perspective of network synchronization [20,21]. For instance, the master stability function (MSF) [22] and the mixed graph stability method [23] are two well-known methods that are proposed to investigate the synchronizability of the dynamical network from an analytical point of view. The local-order parameter is another index that measures the synchrony among the coupled oscillators in the network [24]. Sun et al. [25] have investigated the burst transition in the neural network from the simulation point of view. Plotnikov et al. [26] have considered a heterogeneous FHN neural network with different topologies and have reached the synchronization state by designing a proper controller. Masoliver et al. [27] have reported the effect of time-delay on synchronizing the network consisting of the FHN neuron model. The synchronization of fractional-order FHN neural network has been investigated by Yong et al.'[28]. Moreover, Ma et al. [29] have reported the impact of field and electromagnetic induction on synchronization and wave propagation in neural network.

Local synchronization or emerging chimera state in the dynamical network is the other highlighted collective behavior. In the chimera case, the network is divided into some subgroups with both synchronous and asynchronous behaviors. Various researches in the literature have reported the chimera state in a different field [30]. For instance, Awal et al. [31] reported the smallest chimera state in a pair of coupled chemical oscillators. In [32], the emergence of the chimera state has been explored in coupled pendulums. Böhm et al. [33] explored the chimera states in globally coupled laser networks. Kundu et al. [34] studied the chimera states in an ecological multiplex network. Chimera state is widely investigated in computational biology, especially in neuroscience [35]. For example, experimental results have shown that chimera-like states can be found in a cat's neural network model [36]. A nonstationary [37], imperfect traveling [38] and alternating [39] chimera patterns have been reported in a neural network consist of HR neuron model. Khaleghi et al. [40] have checked the emergence of the chimera state in a map-based neural network. Also, the effect of different features such as time delay [41], fractional-order [42], multilayer [43] has been investigated on emerging chimera states on neural networks.

In this paper, a small-world network of FHN neuronal models with photocell (i.e., photosensitive neurons) is considered. In the first step, the dynamical properties of a single photosensitive neuron are reviewed. Then, by changing the coupling strength, two types of collective states, namely synchronization and chimera states are investigated. For synchronization state, we use the master stability function approach and also verify the result using numerical simulations. The emer-

gence of the chimera state is also explored and verified using the local-order parameter. Finally, the synchronization and chimera states are also explored using recurrence plot analysis.

2 Photosensitive neuron model

Recently, Liu et al. [14] proposed a new photosensitive neuron model that contains a phototube as an excitable voltage source to an FHN neuron model:

$$\begin{aligned} \dot{x} &= x(1-\xi) - \tfrac{x^3}{3} - y + A\cos(\omega t) \\ \dot{y} &= c(x + a - by) \end{aligned} \tag{1}$$

where A and ω represent the amplitude and frequency of the phototube, respectively. Now, we study the dynamical behavior of this single system. Figure 1 shows the dynamical behavior of Eq. 1 in terms of the time series and phase space plots when the parameters are set to $\xi = 0.175, a = 0.7, b = 0.8, c = 0.1, \omega = 1$ and two different amplitudes $A = 1$ and 1.2.

The results of Fig. 1 show that the model is sensitive to the parameters of the phototube. For instance, changing the amplitude of the excitable voltage source in the Eq. 1 can alter the model's dynamics from chaotic to periodic. Accordingly, the phototube's amplitude A and frequency ω of the model is explored with the help of bifurcation analysis. Figure 2 shows the bifurcation and their corresponding Lyapunov exponent diagrams of the Eq. 1 by changing the parameters, amplitude A and frequency ω.

Figure 2 shows the different complex behavior of the single model by small changes in the value of the amplitude and frequency of the phototube or the voltage source of Eq. 1. According to Fig. 2a, increasing the phototube amplitude influences the membrane voltage directly and increases the amplitude of the membrane potential. While the general trend of Fig. 2c shows that increasing the phototube's frequency ends with lower membrane potential. Lyapunov exponent's diagrams confirm that Eq. 1 can lead to complex dynamics such as periodic or chaotic behaviors. For instance, the largest Lyapunov exponent of the neuron model of Eq. 1 in Fig. 2b is positive for $0.82 < A < 1.01$, which affirms that the system is chaotic in this range of parameter. Also, for $0.88 < \omega < 1.02$ in Fig. 2d, the largest Lyapunov exponent's of the neuron model of Eq. 1 is positive too, and the system is in chaotic state. Further increases in the frequency lead the system to the periodic dynamics.

3 Network model: collective behaviors

To investigate the collective dynamical properties of the photosensitive neuron network, a network with small-world topology, consisting of N coupled neurons, is considered as follows:

$$\dot{\mathbf{x}}_i = F(\mathbf{x}_i) + \sigma \sum_{j=1}^{N} L_{ij}\mathbf{x}_j, \quad i = 1, 2, \ldots, N \tag{2}$$

where x_i shows the vector of the system's variables (x and y), F(.) shows the dynamical function of each photosensitive neurons, σ is the coupling coefficient and $L = [l_{ij}]_{N\times N}$ is the Laplacian matrix of the network topology. The coupling between each node of the network is connected through the first variable of the dynamical system. The local dynamics of each node is represented by Eq. 1. The system parameters are fixed for which the individual system is in a chaotic state (cf. Fig. 1c). The next target is to explore the collective dynamical behaviors by changing the coupling strength σ for $N = 50$ number of nodes. Figure 3 represents the time series, spatiotemporal, and the snapshot of each node in the network for three different coupling strengths.

According to the results shown in Fig. 3, collective behavior can emerge in different coupling strengths. For instance, the network can reach complete synchronization state in which the entire network's oscillators move with the same dynamics. Accordingly, similar time-series are obtained by plotting all the network time-series in one diagram (Fig. 3g). Also, both synchronous and asynchronous behavior can be seen in the network simultaneously (Fig. 3e). In this case, the snapshot of each neuron at $t = 3000$ shows two different behaviors in the networks (Fig. 3f). On the other hand, Fig. 3b shows that each neuron in the network can have different dynamical behavior in time for small coupling strength.

Next, we calculate the critical value of the coupling strength for complete synchronization using the master stability function approach.

3.1 Global synchronization: master stability function approach

To analytically investigate the network's synchronizability and calculate the optimum coupling strength for synchronization, the master stability function (MSF) approach is used. In the first step of the MSF approach,

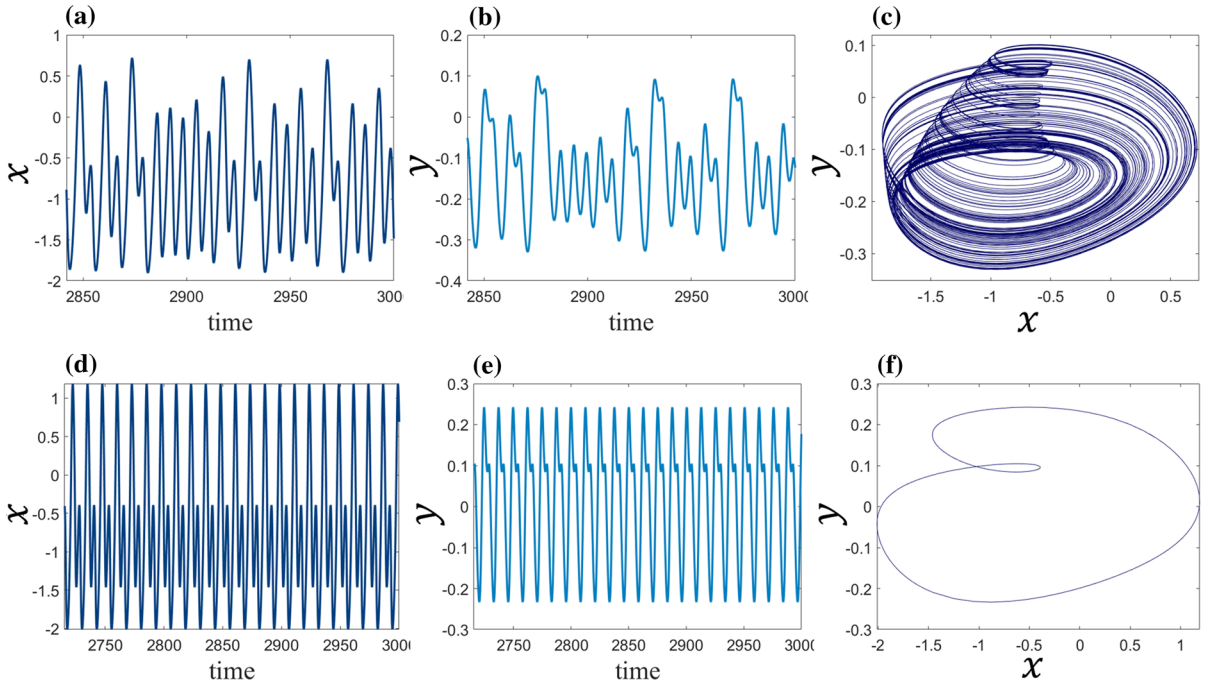

Fig. 1 **a**, **d** Time series of the x-variable which shows the oscillation of neuron voltage with $A = 1$ and 1.2, respectively, **b**, **e** time series of the y-variable for $A = 1$ and 1.2, **c**, **f** the $x - y$ projection of the phase space with $A = 1$ and 1.2 when other parameters are set to $\xi = 0.175, a = 0.7, b = 0.8, c = 0.1, A = 0.9, \omega = 1$ and random initial conditions. The first and second rows show chaotic and periodic behavior for $A = 1$ and 1.2, respectively

it is assumed that the network has a synchronization manifold $s(t)$ in which the dynamics of all the variables of the networks are the same at all times, i.e., $s(t) = x_1(t) = x_2(t) = \cdots = x_N(t)$. The second step is dedicated to calculating the largest Lyapunov exponents of the perturbation equation. The corresponding perturbation equation of the Eq. 2 can be expressed as:

$$\dot{\mathbf{y}}_i = DF(s)\mathbf{y}_i + \sigma\lambda_i\mathbf{y}_i, \tag{3}$$

where D represents the Jacobian matrix and $\lambda_i (i = 1, 2, \ldots, N)$ are the eigenvalues of the L matrix. Figure 4 shows the largest Lyapunov exponent (or the MSF of the network) of Eq. 3 according to different values of the coupling strength σ.

Figure 4 shows the MSF of type-I of the network consists of 50 coupled photosensitive neurons with small-world topology. There is one zero-crossing point in the MSF diagram, which indicates that the network is synchronized for $\sigma \geq 0.589$. However, to explore the network's dynamical behavior before synchronization, the local- and global-order parameters are utilized.

3.2 Chimera states: characterization

Now, we characterize the above obtained chimera states using global-order parameter and recurrence plot analysis.

3.2.1 Global order

The global-order parameter is the spatiotemporal average of the local-order parameters. The global-order parameter is a synchronization index that numerically measures the quantitative range of the synchronization as follows:

$$R = \frac{1}{N}\left|\sum_{k=1}^{N} e^{\sqrt{-1}\theta_k}\right|, \quad \text{where}$$
$$\theta_k = 2\pi\frac{t - t_{k,j}}{t_{k,j+1} - t_{k,j}} \tag{4}$$

where θ_k represent the phase of the kth neuron and the $t_{k,j}$ is the time of jth spike of the kth neuron in the network. Figure 5 shows the global-order parameter

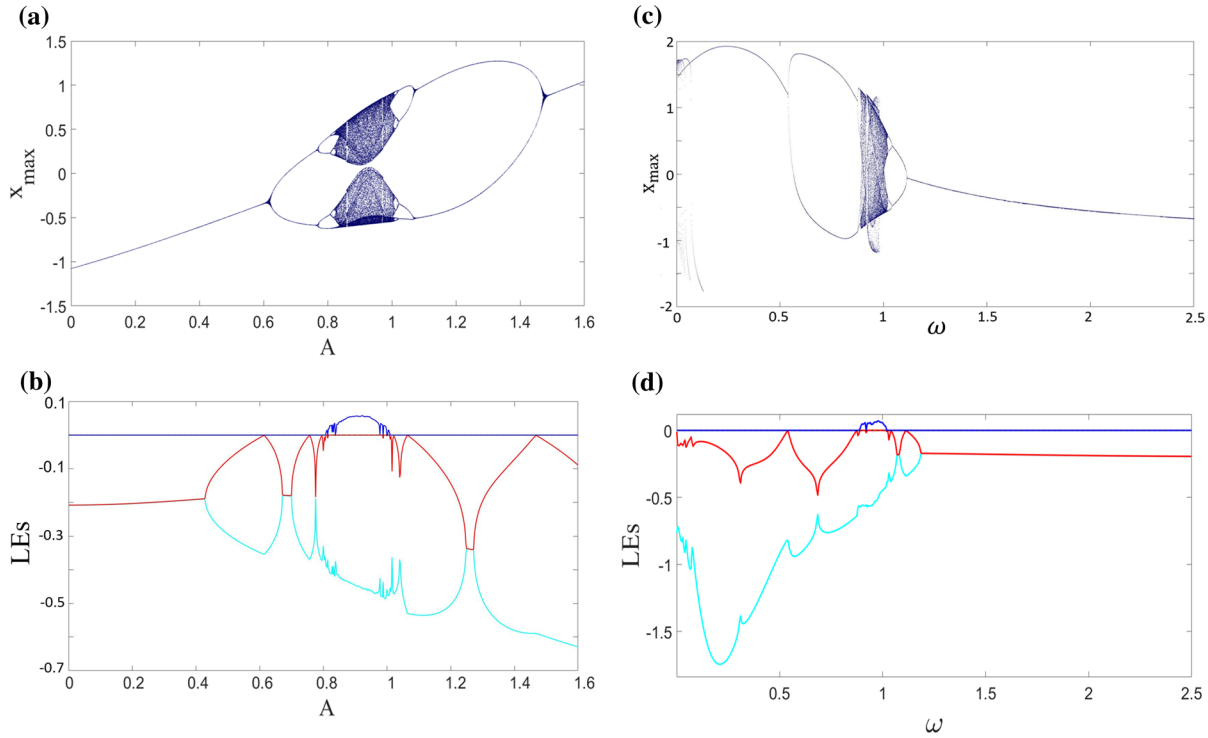

Fig. 2 **a**, **c** Bifurcation diagram and **b**, **d** the corresponding Lyapunov exponents (LEs) diagrams of the Eq. 1 according to changing the phototube's amplitude A and frequency ω when the other parameters are set to $\xi = 0.175, a = 0.7, b = 0.8, c = 0.1$. Period doubling route to chaos is observed in both cases. The maximum Lyapunov exponent is positive in the chaotic regions

according to changing the coupling coefficient in the range $0 \leq \sigma \leq 0.6$.

The increasing trend of the global order parameter indicates that the network's synchronization is increased by increasing the coupling strength, and the network can be fully synchronized for the coupling strength of more than 0.6. Also, the global-order parameter in Fig. 5 shows a local minimum of around $0.04 \leq \sigma \leq 0.085$ in which, unlike the network's global trend, the degree of synchronization decreases, while the coupling strength is increased. This local minimum can be the best candidate for emerging the chimera state in the network. This type of behavior is also observed in heterogeneous Kuramoto network model with attractive and repulsive couplings [44].

Figure 6 shows the network dynamics with different values of the coupling strength in the range of $0.04 \leq \sigma \leq 0.085$. Figure 6 shows five examples of the emergence of chimera state in the network when the coupling strength is chosen in the range $0.04 \leq \sigma \leq 0.085$. Comparing both one-to-one correspondence plots of the first and second rows of Fig. 6 indicates the existence of both synchronous and asynchronous behavior of the network simultaneously. According to all the spatiotemporal plots, local order, and the snapshot at $t = 500$, both coherent and incoherent behaviors exist simultaneously, clarifying the occurrence of chimera state in the network in this specific range of coupling strength.

3.2.2 Recurrence plot

Also, the recurrence quantification analysis is implemented to test the numerical results of Fig. 6. The recurrent plots are virtualization of the network's spatiotemporal behavior that visits the same region of the phase space. The recurrent analysis can be calculated as:

$$\mathrm{RP}_{ij} = \|x_i - x_j\| \quad \text{for} \quad i, j = 1, \ldots, N, \tag{5}$$

where N is the number of nodes and $\|.\|$ is the Euclidean distance. Figure 7 shows the recurrent plots for different values of the coupling strength σ.

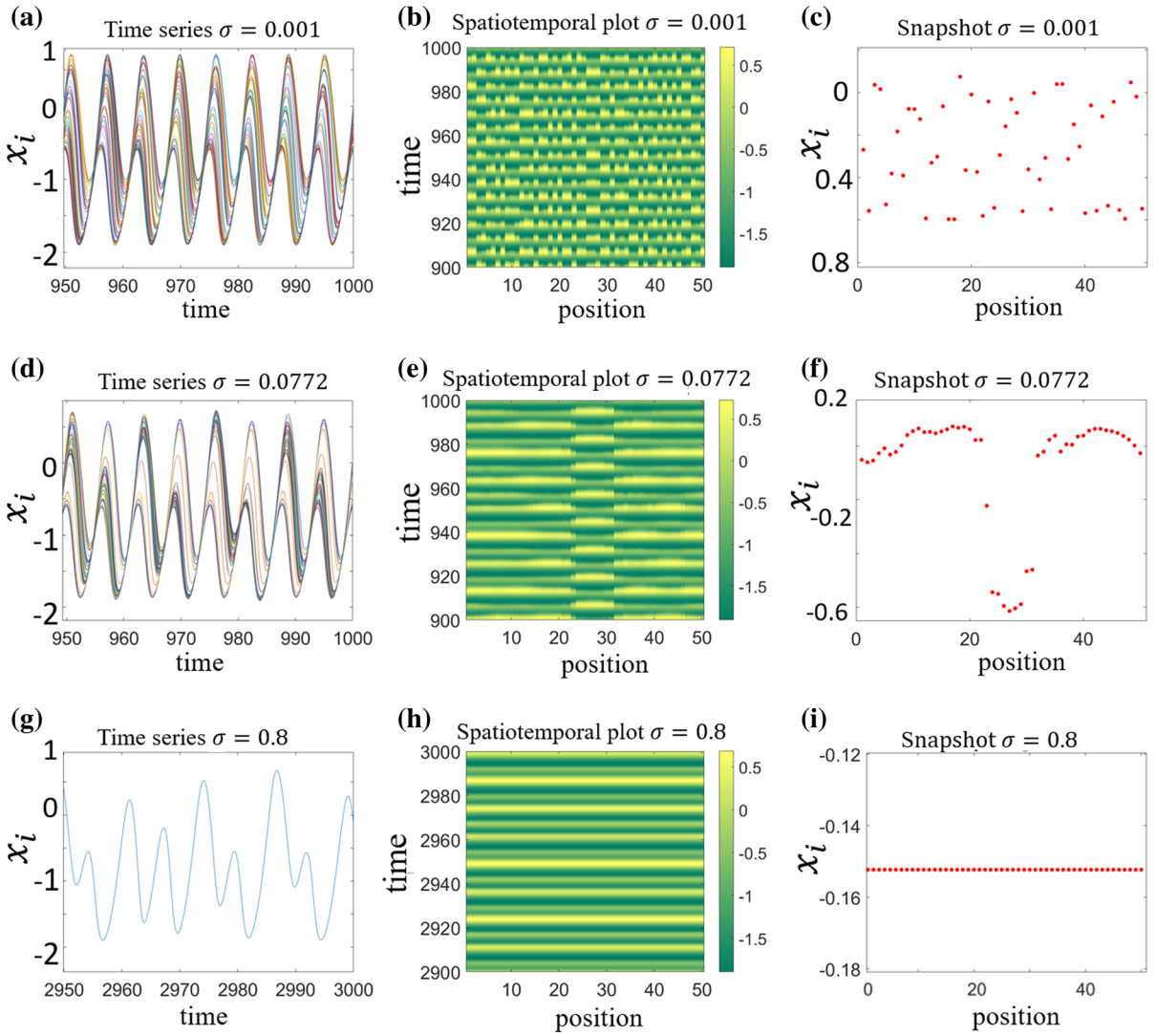

Fig. 3 **a**, **d**, **g** Time series, **b**, **e**, **h** spatiotemporal, and **c**, **f**, **i** snapshot of the state variable x of each neuron in three different coupling strengths $\sigma = 0.001$, 0.0772, and 0.8, respectively. The other parameters are $\xi = 0.175$, $a = 0.7$, $b = 0.8$, $c = 0.1$, $\omega = 1$, and $A = 1$. By changing the coupling strength σ, complete synchronization emerges in the network for higher values of the coupling strength

The incoherent behavior of the network without any structures is shown in Fig. 7a when the coupling strength is set to $\sigma = 0$. In Fig. 7b–e, there are structures in the recurrent plots that indicate the emergence of the chimera states with both synchronous and asynchronous network behavior simultaneously. According to the color box, the blue regions show the synchronized oscillators and the red regions indicate the oscillators with asynchronous behavior. The united recurrent plot of Fig. 7f reveals the network's full synchronous behavior. Relying on the accurate results of Fig. 7 which represented the chimera states' existence distinctly, the recurrence plot is also used as a useful tool in the next section.

3.2.3 Effect of the amplitude of the phototube on the emergence of chimera state

The neuron model's different dynamical behavior is represented as a bifurcation diagram in Fig. 2a accord-

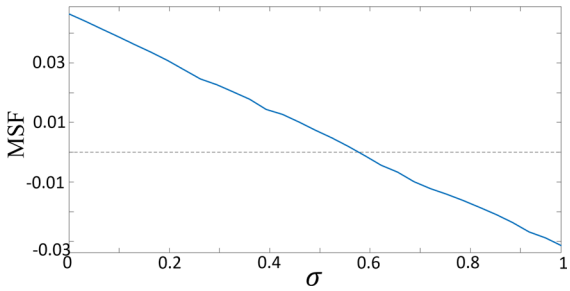

Fig. 4 MSF diagram of the network with respect to the coupling coefficient σ. The MSF of the network is negative for $\sigma \geq 0.589$ when the other parameters are at $\xi = 0.175, a = 0.7, b = 0.8, c = 0.1, \omega = 1$, and $A = 1$

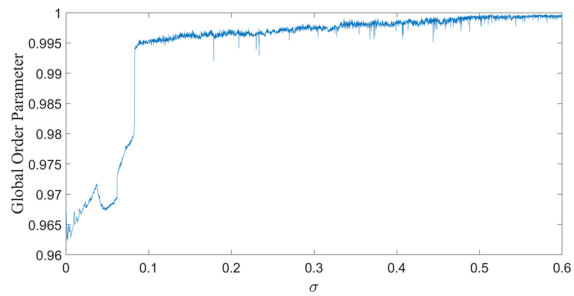

Fig. 5 Global-order parameter of the network for different coupling coefficients for the parameters $\xi = 0.175, a = 0.7, b = 0.8, c = 0.1, \omega = 1$, and $A = 1$

ing to changing the value of the phototube's amplitude. The photosensitive neuron model is chaotic for $0.82 < A < 1.01$, while it is periodic for out of this range. It can be concluded that the phototube's amplitude can affect the response of the photosensitive single neuron. Accordingly, the influence of the phototube's amplitude is explored on the chimera states in the 50 photosensitive coupled neurons. Figure 8 shows the global-order diagram of the network at different coupling strengths.

According to Fig. 8, the network's synchronization states happen in a small value of the coupling strength when each neuron's dynamics are periodic (red and blue lines). However, for each individual's complex behavior in the network, the synchronization happens with more cost, i.e., with higher coupling strengths. The chimera states emerge in the network for a larger value of the coupling strength. Figure 9 shows the emergence of the chimera states for different values of the phototube's amplitude A.

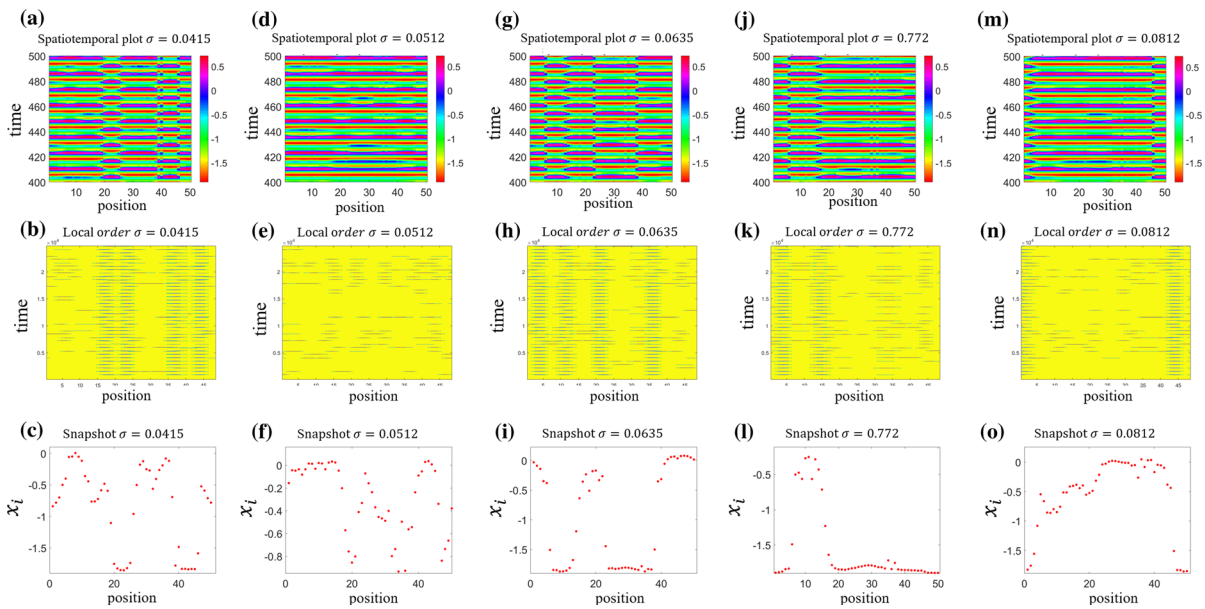

Fig. 6 **a**,**d**,**g**,**j**,**m** Spatiotemporal plots, **b**,**e**,**h**,**k**,**n** local order parameter, and **c**,**f**,**i**,**l**,**o** snapshot at time $t = 500$ of each neuron for five different coupling strengths $\sigma = 0.0415, 0.0512, 0.0615, 0.0772$, and 0.0812, respectively. The other parameters are set to $\xi = 0.175, a = 0.7, b = 0.8, c = 0.1, \omega = 1$, and $A = 1$

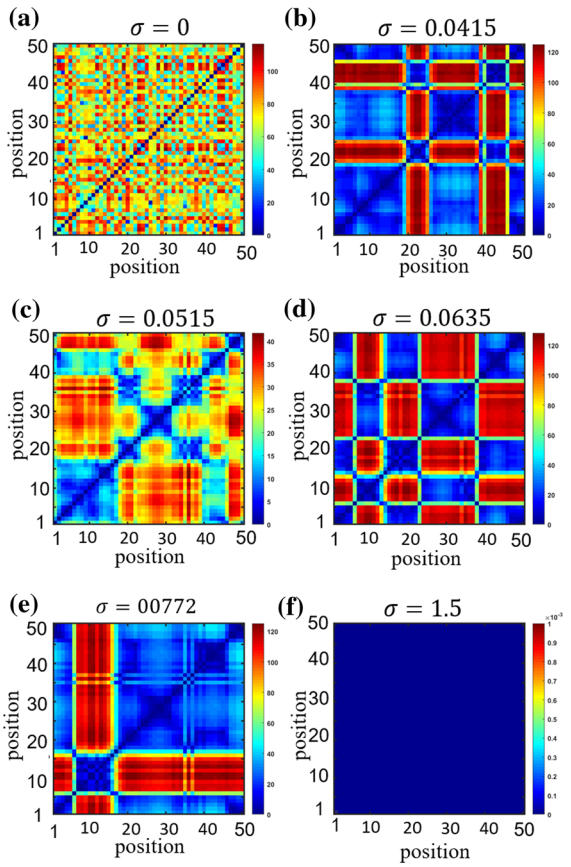

Fig. 7 Recurrence plot of the network for different coupling strengths σ. **a** Incoherent behavior at $\sigma = 0$, **b**,**c**,**d**,**e** chimera states with different structures at $\sigma = 0.0415, 0.0512, 0.0615,$ and 0.077, respectively, and **f** global synchronization at $\sigma = 1.5$

Spatiotemporal pattern, local order parameter, and recurrence plot of the network are used to explore the network's transient dynamical behavior for four different phototube's amplitude at different coupling strengths. The results shown in Fig. 9 reveal that the complex behavior of the phototube can affect the collective patterns of the network. For the chaotic behavior of the photosensitive neuron ($A = 0.85$ and 0.9), the chimera states emerge in the network with the larger value of the coupling strength than the periodic behavior of the photosensitive neuron ($A = 0.7$ and 1.1). For instance, the chimera state emerges in the network with $A = 0.9$ for coupling strength $\sigma = 0.175$. In comparison, the network with $A = 0.7$, the chimera state occurs at $\sigma = 0.0135$. The results clarified that the phototube amplitude directly affects each neuron's dynamics, and complex behavior running in each node can affect the global network's spatiotemporal behavior.

4 Discussion

In this paper, the collective behavior of the photosensitive neuron model was investigated. The excitability of these neurons is triggered with light which is modeled with a time-varying voltage source. At first, it was stated that the values of amplitude and frequency of the phototube can change the dynamics of the neuron model. The time series and state-space of the neuron model are plotted in two different values of the amplitude, which resulted in two different, chaotic and periodic, behaviors. To investigate the single neuron model's sensitivity to phototube parameters, the different complex behavior of the single model was explored with the help of bifurcation diagrams. According to the bifurcation diagrams and their corresponding Lyapunov exponent's diagrams, the single neuron model can produce different complex behaviors such as chaotic and periodic behavior. Moreover, increasing the phototube amplitude influenced the membrane voltage directly and increased the amplitude of the membrane potential. The general trend of the bifurcation diagram of the model according to changing the frequency of the phototube showed that increasing the phototube's frequency ends with lower membrane potential.

After that, a dynamical network consisting of 50 photo-sensitive neuron models was constructed. All the phototubes in the network interacted with each other through Watts–Strogatz small-world topology with $p = 0.09$. The numerical simulations revealed that this network is capable of emerging different collective behaviors such as synchronization and chimera states.

The master stability approach was used to investigate the synchronizability of the network in different coupling strengths. The results showed that the synchronizability of this network belongs to the networks with a type-I MSF diagram. Therefore, the network can be fully synchronized for $\sigma > 0.589$.

The local–global-order parameter and recurrence plot analysis were implemented to investigate the emergence of the chimera states in the network. Both simulation and analytical results confirm that the specific range of the coupling strength and amplitude of the phototube can lead the network to the chimera

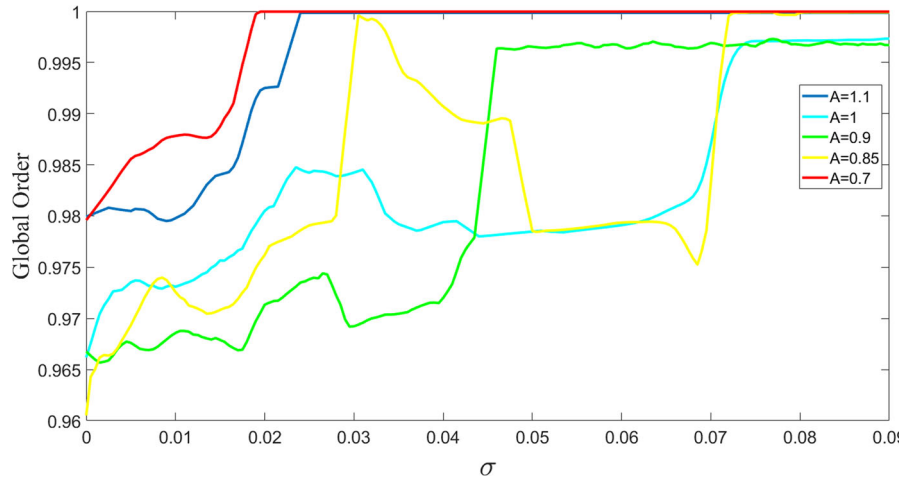

Fig. 8 Global-order parameter of the network for different phototube's amplitude by varying the coupling strength σ. The red, yellow, green, cyan and blue line correspond to the $A = 0.7, 0.85, 0.9, 1.0$ and 1.1, respectively. In this range of coupling strength σ, the network becomes coherent when each neuron is in periodic state

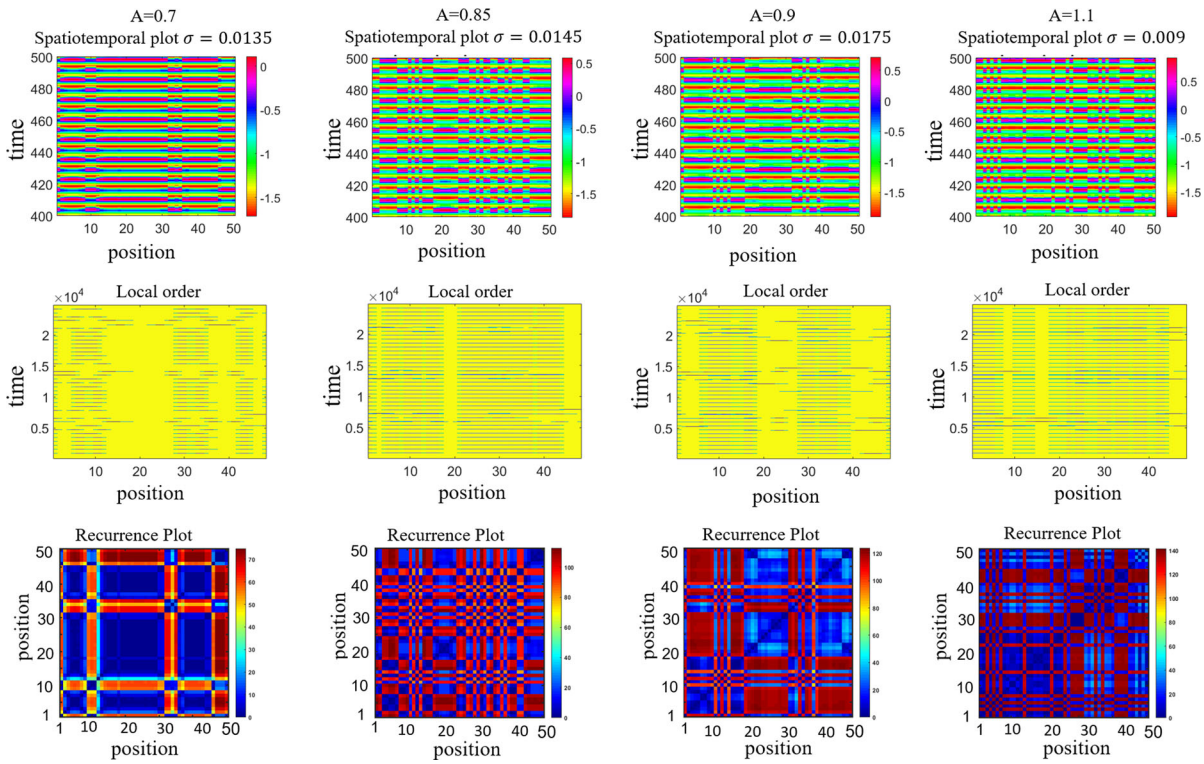

Fig. 9 First row: Spatiotemporal plots, second row: local order parameter, and third row: recurrence plot at four different phototube's amplitude $A = 0.7, 0.85, 0.9$ and 1.1, respectively. The other parameters are set to $\xi = 0.175, a = 0.7, b = 0.8, c = 0.1$, and $\omega = 1$. The respective coupling strengths for each column are $\sigma = 0.0135, 0.0145, 0.0175$, and 0.009

states. According to the results, the chimera states can emerge in the network for the coupling strength range of $0.04 \leq \sigma \leq 0.085$. Also, the phototube amplitude can be considered an effective parameter in the emergence of the chimera states. The results revealed that for the chaotic behavior of the photo-sensitive neuron, the chimera states emerge in the network with the larger value of the coupling strength in comparison with the periodic behavior.

It is worthy of mentioning that the collective behavior of the network of interactive coupled photosensitive neurons can be investigated considering the effect of noise, different kind of synapses such as chemical, otaps, and also electromagnetic synapses, in future researches.

5 Conclusion

Previous studies reveal that a neuron's excitability can be affected by different factors such as voltage, temperature, sound, and optical signals. Recently, a computational model of a photosensitive neuron has been proposed. In this paper, a dynamical network consists of 50 coupled photosensitive neurons with small-world topology is considered. The synchrozability of the network is investigated with the help of the MSF approach. According to the type-I MSF diagram of the network, which contains one zero-crossing point, the optimum coupling of complete synchronization is reported. Furthermore, the emergence of the chimera state is studied considering local- and global-order parameters. The recurrence quantification analysis is also utilized to clarify the numerical results. The chimera state can emerge in the network at the specific range of coupling strength.

Acknowledgements Matjaž Perc was supported by the Slovenian Research Agency (Grant Nos. P1-0403 and J1-2457). S. Jafari is also partially funded by Center for Nonlinear Systems, Chennai Institute of Technology, India vide funding number CIT/CNS/2020/RD/065.

Declarations

Conflict of interest The authors declare no conflict of interest.

References

1. Hall, J.E., Hall, M.E.: Guyton and Hall Textbook of Medical Physiology E-Book. Elsevier Health Sciences (2020)
2. Ma, J., Yang, Z.Q., Yang, L.J., Tang, J.: A physical view of computational neurodynamics. J. Zhejiang Univ. Sci. A **20**(9), 639 (2019)
3. Ma, J., Tang, J.: A review for dynamics in neuron and neuronal network. Nonlinear Dyn. **89**(3), 1569 (2017)
4. Hodgkin, A.L., Huxley, A.F.: A quantitative description of membrane current and its application to conduction and excitation in nerve. J. Physiol. **117**(4), 500 (1952)
5. Hindmarsh, J.L., Rose, R.: A model of neuronal bursting using three coupled first order differential equations. Proc. R. Soc. Lond. B **221**(1222), 87 (1984)
6. FitzHugh, R.: Mathematical models of threshold phenomena in the nerve membrane. Bull. Math. Biophys. **17**(4), 257 (1955)
7. Uzuntarla, M., Ozer, M., Ileri, U., Calim, A., Torres, J.J.: Effects of dynamic synapses on noise-delayed response latency of a single neuron. Phys. Rev. E **92**(06), 062710 (2015)
8. Valenti, D., Augello, G., Spagnolo, B.: Dynamics of a FitzHugh–Nagumo system subjected to autocorrelated noise. Eur. Phys. J. B **65**(3), 443 (2008)
9. Hou, Z., Ma, J., Zhan, X., Yang, L., Jia, Y.: Estimate the electrical activity in a neuron under depolarization field. Chaos Solitons Fractals **142**, 110522 (2020)
10. Yan, B., Panahi, S., He, S., Jafari, S.: Further dynamical analysis of modified Fitzhugh–Nagumo model under the electric field. Nonlinear Dyn. **101**(1), 521 (2020)
11. Xu, Y., Jia, Y., Ma, J., Hayat, T., Alsaedi, A.: Collective responses in electrical activities of neurons under field coupling. Sci. Rep. **8**(1), 1349 (2018)
12. Feng, P., Wu, Y., Zhang, J.: A route to chaotic behavior of single neuron exposed to external electromagnetic radiation. Front. Comput. Neurosci. **11**, 94 (2017)
13. Uzuntarla, M., Ozer, M., Guo, D.: Controlling the first-spike latency response of a single neuron via unreliable synaptic transmission. Eur. Phys. J. B **85**(8), 1 (2012)
14. Liu, Y., Xu, W.J., Ma, J., Alzahrani, F., Hobiny, A.: A new photosensitive neuron model and its dynamics. Front. Inf. Technol. Electron. Eng **21**, 1387 (2020)
15. Calim, A., Torres, J.J., Ozer, M., Uzuntarla, M.: Chimera states in hybrid coupled neuron populations. Neural Netw. **126**, 108 (2020)
16. Reinhart, R.M., Nguyen, J.A.: Working memory revived in older adults by synchronizing rhythmic brain circuits. Nat. Neurosci. **22**(5), 820 (2019)
17. Babiloni, C., Lizio, R., Marzano, N., Capotosto, P., Soricelli, A., Triggiani, A.I., Cordone, S., Gesualdo, L., Del Percio, C.: Brain neural synchronization and functional coupling in Alzheimer's disease as revealed by resting state EEG rhythms. Int. J. Psychophysiol. **103**, 88 (2016)
18. Calim, A., Hövel, P., Ozer, M., Uzuntarla, M.: Chimera states in networks of type-I Morris–Lecar neurons. Phys. Rev. E **98**, 062217 (2018)
19. Xu, Y., Jia, Y., Ma, J., Alsaedi, A., Ahmad, B.: Synchronization between neurons coupled by memristor. Chaos Solitons Fractals **104**, 435 (2017)
20. Nazarimehr, F., Panahi, S., Jalili, M., Perc, M., Jafari, S., Ferčec, B.: Multivariable coupling and synchronization in complex networks. Appl. Math. Comput. **372**, 124996 (2020)
21. Rakshit, S., Bera, B.K., Bollt, E.M., Ghosh, D.: Intralayer synchronization in evolving multiplex hypernetworks: analytical approach. SIAM J. Appl. Dyn. Syst. **19**(2), 918 (2020)
22. Pecora, L.M., Carroll, T.L.: Master stability functions for synchronized coupled systems. Phys. Rev. Lett. **80**(10), 2109 (1998)
23. Belykh, V.N., Belykh, I.V., Hasler, M.: Connection graph stability method for synchronized coupled chaotic systems. Physica D **195**(1), 159 (2004)
24. Omel'chenko, E., Sebek, M., Kiss, I.Z.: Universal relations of local order parameters for partially synchronized oscillators. Phys. Rev. E **97**(6), 062207 (2018)

25. Sun, X., Lei, J., Perc, M., Kurths, J., Chen, G.: Burst synchronization transitions in a neuronal network of subnetworks. Chaos **21**(1), 016110 (2011)
26. Plotnikov, S., Lehnert, J., Fradkov, A., Schöll, E.: Synchronization in heterogeneous FitzHugh–Nagumo networks with hierarchical architecture. Phys. Rev. E **94**(1), 012203 (2016)
27. Masoliver, M., Malik, N., Schöll, E., Zakharova, A.: Coherence resonance in a network of FitzHugh–Nagumo systems: interplay of noise, time-delay, and topology. Chaos **27**(10), 101102 (2017)
28. Liu, Y., Xie, Y.: Dynamical characteristics of the fractional-order FitzHugh–Nagumo model neuron and its synchronization. Acta Phys. Sin. **59**(3), 2147 (2010)
29. Ma, J., Wu, F., Hayat, T., Zhou, P., Tang, J.: Electromagnetic induction and radiation-induced abnormality of wave propagation in excitable media. Physica A **486**, 508 (2017)
30. Majhi, S., Bera, B.K., Ghosh, D., Perc, M.: Chimeras at the interface of physics and life sciences: reply to comments on Chimera states in neuronal networks: a review. Phys. Life Rev. **28**, 142 (2019)
31. Awal, N.M., Bullara, D., Epstein, I.R.: The smallest chimera: periodicity and chaos in a pair of coupled chemical oscillators. Chaos **29**(1), 013131 (2019)
32. Wojewoda, J., Czolczynski, K., Maistrenko, Y., Kapitaniak, T.: The smallest chimera state for coupled pendula. Sci. Rep. **6**(1), 34329 (2016)
33. Böhm, F., Zakharova, A., Schöll, E., Lüdge, K.: Amplitude-phase coupling drives chimera states in globally coupled laser networks. Phys. Rev. E **91**(4), 040901 (2015)
34. Kundu, S., Majhi, S., Ghosh, D.: From asynchronous to synchronous chimeras in ecological multiplex network. Eur. Phys. J. Spec. Top. **228**(11), 2429 (2019)
35. Parastesh, F., Jafari, S., Azarnoush, H., Shahriari, Z., Wang, Z., Boccaletti, S., Perc, M.: Chimeras. Phys. Rep. (2020)
36. Santos, M., Szezech, J., Borges, F., Iarosz, K., Caldas, I., Batista, A., Viana, R., Kurths, J.: Chimera-like states in a neuronal network model of the cat brain. Chaos Solitons Fractals **101**, 86 (2017)
37. Bera, B.K., Rakshit, S., Ghosh, D., Kurths, J.: Spike chimera states and firing regularities in neuronal hypernetworks. Chaos **29**(5), 053115 (2019)
38. Bera, B.K., Ghosh, D., Banerjee, T.: Imperfect traveling chimera states induced by local synaptic gradient coupling. Phys. Rev. E **94**(1), 012215 (2016)
39. Majhi, S., Ghosh, D.: Alternating chimeras in networks of ephaptically coupled bursting neurons. Chaos **28**(8), 083113 (2018)
40. Khaleghi, L., Panahi, S., Chowdhury, S.N., Bogomolov, S., Ghosh, D., Jafari, S.: Chimera states in a ring of map-based neurons. Physica A **536**, 122596 (2019)
41. Bera, B.K., Ghosh, D.: Chimera states in purely local delay-coupled oscillators. Phys. Rev. E **93**(5), 052223 (2016)
42. He, S.: Complexity and chimera states in a ring-coupled fractional-order memristor neural network. Front. Appl. Math. Stat. **6**, 24 (2020)
43. Majhi, S., Perc, M., Ghosh, D.: Chimera states in a multilayer network of coupled and uncoupled neurons. Chaos **27**(7), 073109 (2017)
44. Frolov, N., Maksimenko, V., Majhi, S., Rakshit, S., Ghosh, D., Hramov, A.: Chimera-like behavior in a heterogeneous Kuramoto model: the interplay between attractive and repulsive coupling. Chaos **30**(8), 081102 (2020)